Synthesis of ≈10 Å Thiophenolate-capped CdS Clusters. Observation of a Sharp Absorption Peak†

Norman Herron,* Andris Suna* and Ying Wang*
Central Research and Development Department, E. I. du Pont de Nemours & Company, Wilmington, DE 19880-0328, USA

The controlled growth of semiconductor clusters from a precursor phenyl-capped CdS molecule, $[Cd_{10}S_4(SPh)_{16}]^{4-}$, by the addition of stoichiometric amounts of sulfide ion has led to a material having a sharp (full width at half-maximum at room temperature ≈800 cm^{-1}) excitonic feature at 351 nm (3.53 eV) in its absorption spectrum. This narrow spectral feature, coupled with the synthetic conditions necessary to produce it and the chemical stoichiometry, suggests a very narrowly dispersed, anionically charged, pyramidal-shaped cluster of around 10 Å diameter and composed of ≈55 atoms in a tetrahedral (sphalerite) arrangement (by analogy with the starting material structure). Computer simulation shows that the X-ray powder diffraction data are consistent with this hypothetical pyramidal structure. A simple tight-binding (Hückel) model, fitted to the bulk band structure, is used to describe the energy levels in such a cluster; the lowest calculated transition, after perturbation by the Coulomb interaction, displays an isolated peak at 3.66 eV, close to the observed value. The wavefunctions of the hole and electron calculated from the model reveal the hole largely located at the central S atom of the cluster and the electron delocalized over the surrounding 16 Cd atoms.

A key objective of research in the area of small semiconductor clusters is to produce such species in a very narrow size dispersion. Such a material would permit the examination of intrinsic optical and other physical properties of a given cluster dimension unclouded by the averaging effects of having an inhomogeneous distribution of cluster sizes. While many techniques have been developed for the synthesis of small particulate semiconductor clusters[1] almost all produce a significant size dispersion. Our previous work on extremely small CdS clusters in zeolite Y[2,3] is one of the very few where a unique cluster size and geometry have been determined and the resultant physical properties examined. In this case, however, the clusters are co-ordinated strongly to the matrix *via* cadmium–zeolite oxygen bonding and have a basic structure (cubane) quite unlike the bulk semiconductor itself (sphalerite). We have recently begun to explore the use of organic capping of CdS clusters[4] and our work builds upon the ideas set forth by a number of other research groups.[5–8] Our method can be likened to an inorganic polymerization reaction where the extent of polymerization (chain length) is controlled by adding a growth-inhibitor molecule, in this case the surface-cap thiophenolate ion. During our investigations we noted that this reaction in some ways mirrored a living polymerization since further sulfide ion/cadmium ion additions would allow the cluster growth to resume. While this approach has resulted in a method for producing a size-graded series of soluble clusters, the products still suffer the problem of being a dispersion of sizes within each individual preparation. We now report a method for growing a very narrow size-dispersed cluster from a molecular precursor by controlled sulfide addition, making use of the 'living polymerization' analogy, and an examination of the optical properties of the resultant material.

Experimental

Cadmium acetate, thiophenol and sodium sulfide (anhydrous) were used as received from Alfa Chemical. Chemical analyses using combustion (C + H) and atomic absorption were performed by Galbraith, Knoxville, TN. X-Ray powder diffraction measurements were performed on a Scintag automated powder diffractometer using Cu-Kα radiation. Electronic spectra were taken in 1 mm pathlength quartz cells using a Perkin Elmer 559 UV/VIS spectrophotometer. Photoluminescence spectra were taken on a Spex Fluorolog fluorimeter. All the reported spectra have been corrected for the photomultiplier response. Samples were cooled in a continuous-flow helium cryostat (Oxford Instruments CF1204). All synthetic procedures and sample manipulations were carried out in an inert-atmosphere (nitrogen) dry-box from Vacuum Atmospheres (<10 ppm oxygen, <10 ppm water). Solvents for synthesis and optical measurements were dried and deoxygenated by standard techniques.

Cluster Preparation.—The compound $[NMe_4]_4[Cd_{10}S_4(SPh)_{16}]$ **1** was prepared in the glove-box following the published procedure[5] and was recrystallized from acetonitrile as large colourless crystals. It (0.0825 g, 2.5×10^{-5} mol) was dissolved in dry, deaerated dimethylformamide (dmf) (50 cm^3) and stirred vigorously with a magnetic stirrer. A second solution of anhydrous sodium sulfide (0.039 g) in a mixed solvent of water (2 cm^3) and dmf (8 cm^3, 5×10^{-2} mol dm^{-3}) was prepared and stirred until clear and homogeneous. This sulfide solution (1.25 cm^3, 6.25×10^{-5} mol) was added to the stirred solution of compound **1** which remains colourless and clear. After stirring for 5 min, the solution contains the cluster species with the sharp exciton feature at 351 nm which may be observed by recording an electronic spectrum in a 1 mm pathlength cell. The cluster was isolated by evaporation of the solution to dryness at room temperature in a vacuum. The resultant off-white powder may be washed with methanol to remove sodium- and tetramethylammonium-thiophenolate by-products and redissolved in dmf or dmf–2-methyltetrahydrofuran for further optical characterization (Found: C, 31.60; H, 3.20; Cd, 44.25; N, 1.40; S, 19.65. Calc. for $C_{134}H_{155}Cd_{20}N_5S_{32}$: C, 31.5; H, 3.05; Cd, 44.00; N, 1.35; S, 20.10%).

† *Non-SI unit employed:* eV ≈ 1.60×10^{-19} J.

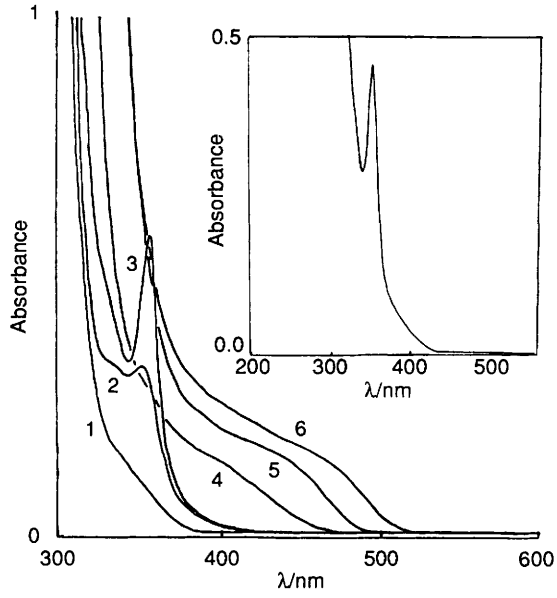

Fig. 1 Electronic spectra showing the titration of sulfide ion into a dmf solution of $[Cd_{10}S_4(SPh)_{16}]^{4-}$ (1.25×10^{-4} mol dm^{-3}) in 1 mm pathlength cells. Ratio of cluster to added sulfide: 1, 1:0; 2, 1:1; 3, 1:2.5; 4, 1:4; 5, 1:10; 6, 1:20. The inset shows the spectrum at the titration ratio of 1:2.5

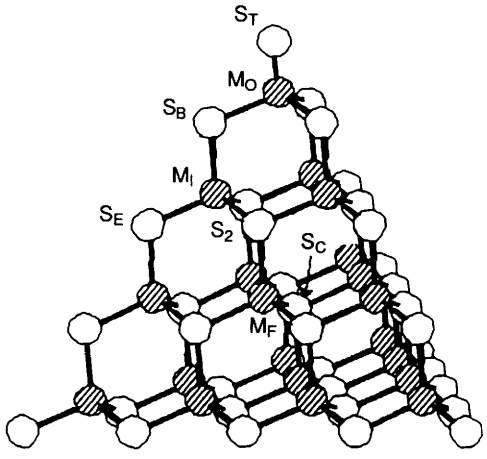

Fig. 2 Idealized pyramidal structure of the 55-atom cluster, $[Cd_{20}S_{13}(SPh)_{22}]^{8-}$: M represents cadmium and S sulfur atoms

Results and Discussion

Cluster Synthesis.—The seminal work of Dance *et al.*[5] on small molecular clusters of CdS led us to explore the use of thiophenol as a capping agent for the controlled growth of larger CdS clusters in the 10–100 Å range.[4] Our method of mixing cadmium ions and sulfide ions in the presence of thiophenolate ions may, as noted previously, be likened to an inorganic polymerization. While this approach was very successful in producing size-graded, soluble CdS fragments in a variety of solvents, all materials prepared by this route appear to be mixtures of a variety of capped-cluster sizes. The size dispersion of these mixtures is enough to smear out the sharp excitonic absorption peak expected from monodisperse clusters. It has, therefore, become our goal to produce a monodispersed cluster size, a larger homologue of the end member $[Cd_{10}S_4(SPh)_{16}]^{4-}$ prepared by Dance. The approach adopted has been to try to grow larger homologues from the Dance material by careful addition of reagents designed to cement together these smaller units.

Using this idea and the observation from our previous work that such clusters can be grown larger simply by addition of extra sulfide ion we explored controlled addition of sulfide ion to the Dance material in dmf solution. The results of such a titration experiment are illustrated in Fig. 1. The sequential addition of extra aliquots of sulfide ion are seen to result in a steady shift in the band-edge absorption onset as would be expected for increasing size of the cluster CdS core. More remarkable, however, is the observation of a very sharp absorption feature at 351 nm (3.53 eV) with a second shoulder at 330 nm at a precise ratio of 2.5 sulfide ions per original $[Cd_{10}S_4(SPh)_{16}]^{4-}$ cluster. This spectrum is featured as an inset in Fig. 1. As more sulfide is titrated into the solution the peak at 351 nm disappears as the clusters continue to grow.

The growth of the sharp peak at 351 nm is extremely sensitive to the concentration of reagents used in the preparation. Lower concentrations (0.1 times those in the Experimental section) result in a broadened peak at 340 nm developing first (minutes) which then very slowly (hours) changes to the peak at 351 nm with no evidence of isosbestic behaviour at any stage of the transformation. With higher reagent concentrations (greater or equal to that in the Experimental section) the sharp peak at 351 nm appears very rapidly (within minutes). We also found that, if the concentration of the species absorbing at 351 nm is increased, the width of the band begins to increase, presumably due to the effects of aggregation. Alternatively, further dilution does not reduce the width beyond that presented in Fig. 1.

When one considers the exact nature and molecularity of the transformation in the present case, that is $[Cd_{10}S_4(SPh)_{16}]^{4-}$ and S^{2-} ions mixed in the ratio 1:2.5, one is tempted to interpret the species absorbing at 351 nm as the next largest homologue of the original Dance cluster, where one extra sphalerite layer has been added to the tetrahedral cluster. Such a species is predicted[5] to have a formulation of $[Cd_{20}S_{13}(SPh)_{22}]^{8-}$ so that the synthesis equation (1) may be

$$2[Cd_{10}S_4(SPh)_{16}]^{4-} + 5S^{2-} \longrightarrow [Cd_{20}S_{13}(SPh)_{22}]^{8-} + 10SPh^{-} \quad (1)$$

written. This reaction can therefore be considered as the fusing of two small clusters, using sulfide ions as the 'cement', to form a larger cluster. Even a cursory consideration of a possible mechanism for such a transformation makes it clear that major reorganization of the original cluster has to take place and, as we observed, the kinetics should be very sensitive to the concentrations of the reagents used.

Whereas the idealized product of this cluster-fusion reaction has the formula $[Cd_{20}S_{13}(SPh)_{22}]^{8-}$, chemical analysis of the isolated solid product indicates that the cluster is, in fact, slightly deficient in thiophenolate capping ions, having only 19 rather than the required 22. This may be the result of the weak cadmium–thiophenolate bonding coupled with some steric crowding which the thiophenol caps experience when covering the edges of such a small cluster (see structure description below and in Fig. 2).

An idealized $[Cd_{20}S_{13}(SPh)_{22}]^{8-}$ structure is illustrated in Fig. 2. It differs from the starting Dance cluster in that it now contains cadmium ions (four) which are co-ordinated only to four sulfide ions rather than mixed sulfide/thiophenolate ion co-ordination. Likewise the cluster also now contains a sulfide ion (the central one) which is co-ordinated to four cadmium ions. This means that this cluster size is the smallest which has both the sphalerite structure of bulk CdS *and* some of the same co-ordination environments for Cd and S as are observed in bulk CdS. Interestingly, this is also the smallest cluster for which a sharp exciton-like absorption peak is observed. The sphalerite core of such a cluster is estimated to be ≈ 10 Å in diameter. Further characterization of this cluster comes from a detailed analysis of X-ray data now presented below.

X-Ray Diffraction Spectrum.—A solid material can be isolated from solution as a creamy white powder either by evaporation and washing or by precipitation using a non-solvent such as methanol. (The isolated solid may be easily

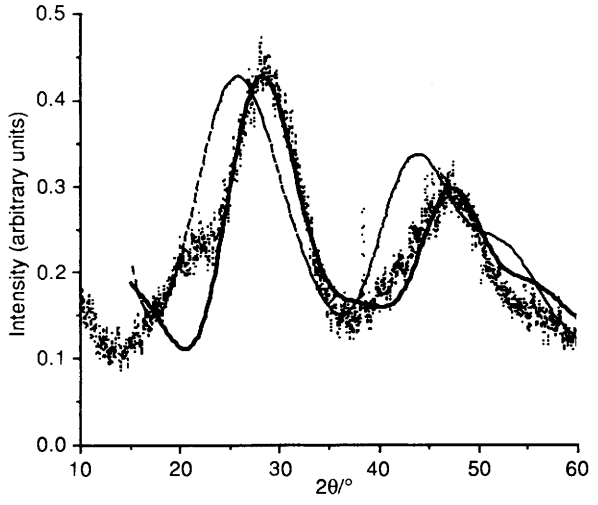

Fig. 3 Powder X-ray diffraction patterns (with Cu-Kα radiation) of the 55-atom CdS cluster (dots). ——, Simulated pattern using parameters given in Table 1, corresponding to a slightly compressed pyramidal structure; – – – –, simulated pattern of the 30-atom cluster, $[Cd_{10}S_4(SPh)_{16}]^{4-}$, using known single-crystal structure data from ref. 5

Table 1 Bond angles (°) and bond lengths (Å) of the proposed 55-atom CdS cluster that give the best fit to the experimental X-ray diffraction pattern

M_O–S_T	2.473	S_C–M_F	2.52
M_O–S_B	2.565	S_2–M_F	2.608
M_I–S_B	2.608	S_E–M_I	2.484
M_I–S_2	2.484		
S_B–M_O–S_T	105.0	M_I–S_2–M_I	103.36
M_I–S_B–M_O	100.0	S_2–M_I–S_2	132.45
S_2–M_I–S_B	100.0	S_B–M_O–S_B	113.55
S_2–M_F–S_2	103.48	S_B–M_I–S_E	95.94
M_I–S_2–M_F	94.76	S_C–M_F–S_2	114.95
M_I–M_E–M_I	92.4		

redissolved in solvents such as dmf, Me_2SO, acetonitrile, *etc.*). Fig. 3 shows its X-ray powder diffraction pattern. The two broad peaks located at 2θ of 28.5 and 47° are characteristic of very small CdS clusters.[4] The first peak is to be compared to the (111) peak of bulk CdS (sphalerite-like phase) located at 26.5°. The weak shoulder at ≈20° may be due to residual thiophenolate salt which is a by-product of the synthetic reaction [see equation (1)] and which is only poorly crystalline (the diffraction pattern of a genuine sample of this material prepared in, and then rapidly precipitated from, dmf solution shows a similar broad amorphous peak at ≈20°); of course many amorphous materials show a broad diffraction peak at this value of 2θ. To gain additional information from these data we have directly simulated the X-ray powder diffractogram of the 30-atom starting cluster and the 55-atom product cluster. For a set of point scatterers located at R_j, each having a scattering amplitude f_j, a simple scalar theory of X-ray diffraction gives expressions (2)–(4) for the X-ray scattering

$$I(2\theta) = \sum_{i,j} f_i f_j [(\sin q \cdot R_{ij})/qR_{ij}] \quad (2)$$

$$R_{ij} \equiv |\vec{R}_i - \vec{R}_j| \quad (3)$$

$$q = \frac{4\pi}{\lambda} \sin\theta \quad (4)$$

pattern, where λ is the X-ray wavelength. Dividing $I(2\theta)$ by sin 2θ gives the experimentally measured scattering intensity for a fixed solid angle $(\sin 2\theta)\delta\theta\delta\varphi$ (where θ and φ define the angle of the diffraction vector in three dimensions using standard conventions). Equation (4) is readily evaluated for a finite cluster with a known set of R_j and f_j. This approach has been used before to simulate cluster X-ray patterns[9] and in the present calculation only the relative value of f_j is required and can be taken as the relative atomic number of the element.

The atomic coordinates of the 30-core-atom cluster $[Cd_{10}S_4(SPh)_{16}]^{4-}$ are known from the single-crystal X-ray diffraction study.[5] The simulated X-ray powder diffraction pattern of the CdS core, displayed as the dashed line in Fig. 3, is clearly different from the experimental data for our new cluster. (Note that the actual diffraction pattern of a genuine sample of the 30-atom cluster is not reproduced by the calculated pattern since the material crystallizes and so is representative of the cluster–cluster crystallinity rather than the individual cluster CdS cores.[5]) This important result eliminates the possibility that the species with the sharp absorption peak at 351 nm may be due to aggregates of the 30-atom cluster, since the powder X-ray diffraction pattern of aggregated 30-atom clusters should be essentially the same as that of a single 30-atom cluster. The 30-atom clusters must fuse together to produce a larger cluster with different atomic arrangements. The synthetic information already presented suggests that this larger cluster may be the 10 Å pyramidal $[Cd_{20}S_{13}(SPh)_{22}]^{8-}$ cluster.

We next simulated the X-ray diffraction pattern of a 55-atom pyramidal cluster. Its hypothetical structure and the labelling of the atoms are shown in Fig. 2. The structure of this cluster is determined by the values of seven bond lengths (*i.e.* M_O–S_T, M_O–S_B, M_I–S_B, M_I–S_2, S_C–M_F, S_2–M_F, S_E–M_I) and three bond angles (*i.e.* S_B–M_O–S_T, M_I–S_B–M_O, S_2–M_I–S_B). To minimize the number of fitting parameters, we have made the assumption that the bond lengths and angles of the 55-atom cluster are the same as those of the 30-atom cluster at the corresponding positions. In this way the number of fitting parameters is reduced to three.

For the bond lengths M_O–S_T, M_O–S_B, M_I–S_B, M_I–S_2, S_2–M_F and S_E–M_I), we use the corresponding values for the 30-atom CdS cluster (Table 1). For the central sulfur atom there is no analogous atom in the 30-atom cluster, and we take the S_C–M_F bond length to be the same as that of bulk CdS (since it has the same sphalerite structure and co-ordination environment), 2.52 Å. The values of the three bond angles were then optimized to give the best fit to the experimental X-ray diffraction pattern. Table 1 lists the bond lengths and angles of the best fit. The simulated diffraction pattern, obtained using these values, is displayed as the solid line in Fig. 3. The agreement between the simulation and experiment is quite good.

The bond lengths and angles given in Table 1 correspond to a slightly 'compressed' or 'rounded' pyramidal structure. The planes consisting of the S_E–M_I–S_2 atoms are pushed towards the centre from the four corners. As a result the bond angles M_I–S_2–M_F, M_I–S_E–M_I and S_B–M_I–S_E approach the value for the rock-salt structure, 90° (although the data cannot be fitted using a simple rock-salt structure). Correspondingly the distance between the cadmium planes shortens which explains the shift of the 2θ value from 26.5 to 28.5°.

We note that the values given in Table 1 should be taken with the understanding that they are derived using the assumption that the 55-atom cluster possesses the same pyramidal structure as that of the 30-atom Dance cluster. This assumption, while appearing reasonable, still needs to be confirmed by future single-crystal studies if such become feasible. The main value of the fitting exercise presented above is two fold: (1) to eliminate the possibility that the sample is simply aggregates of 30-atom clusters; and (2) to show that the powder diffraction data are consistent with the hypothetical pyramidal structure of the 55-atom cluster, inferred from the reaction stoichiometry and chemical analyses. At present we cannot eliminate the possibility that the clusters may have slightly different conformations and/or contain defects, especially in view of the

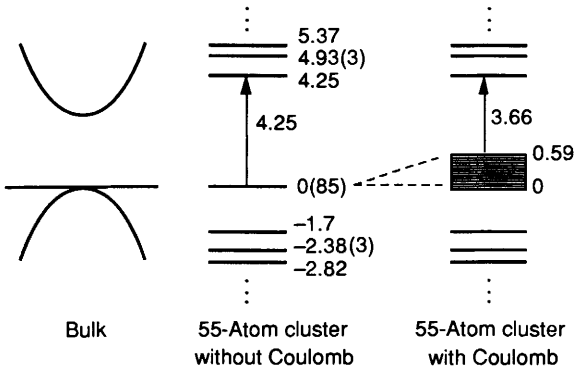

Fig. 4 Left: bulk hexagonal CdS band structure calculated using our simple tight-binding model. Centre: energy levels of the 55-atom CdS cluster, $[Cd_{20}S_{13}(SPh)_{22}]^{8-}$, calculated using the present model without consideration of the Coulomb interaction (the energies are in eV and the numbers in parentheses represents the degeneracy of the level). Right: energy levels of the 55-atom CdS cluster with degenerate perturbation treatment of the Coulomb interaction. The HOMO–LUMO gap is 3.66 eV

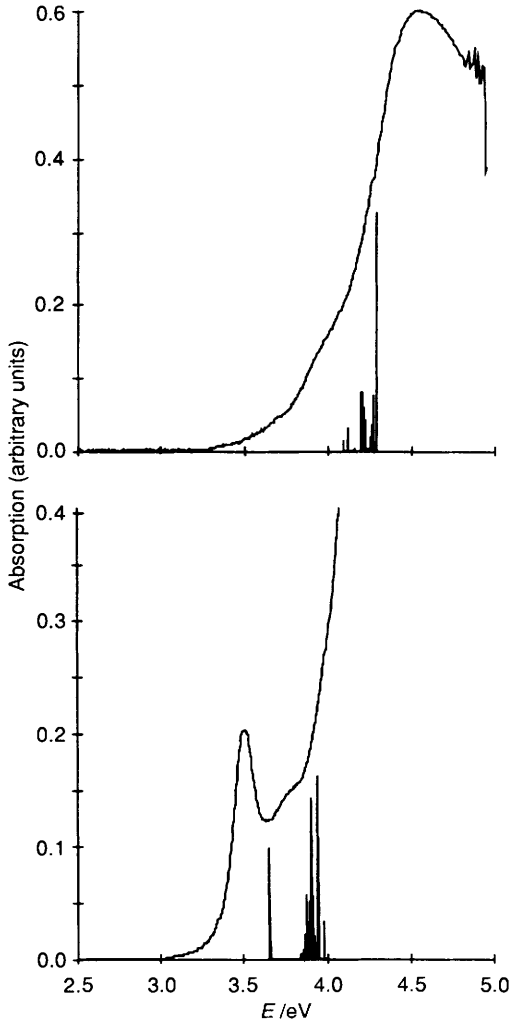

Fig. 5 Comparison between the calculated relative oscillator strengths of the lowest transitions and the experimental absorption spectra for the 30-atom cluster (upper) and the 55-atom cluster (lower)

chemical analysis results which show a slight deficiency of the surface thiophenolate groups.

Tight-binding Calculations.—In this section we develop a simple, tight-binding (Hückel) model for describing the lowest electronic excitations of the tetrahedral 30- and 55-atom clusters. Only Cd and S atoms are considered, the peripheral phenyl groups being ignored. In the following we briefly describe the model and present essential results. The details are presented in the Appendix. Similar tight-binding calculations have been performed previously for PbS[10] and CdS[11] clusters.

The model considers states composed of 3p orbitals on the S atoms and 5s on the Cd. It contains only two adjustable parameters: a Cd to S transfer matrix element, β, and a Cd–S energy difference, Δ. The values of these parameters are chosen to obtain the correct Γ-point effective masses and the energy gap of the bulk hexagonal CdS. As shown in the Appendix, this simple model reproduces the salient features of the energy bands generated by more sophisticated calculation[12] [Fig. 4(left)], including the correct prediction of the relative ratio of the electron and hole effective masses.

The one-electron states of these tetrahedral clusters can be obtained by evaluating a 125 × 125 Hamiltonian for the 55-atom cluster and a 70 × 70 Hamiltonian for the 30-atom cluster. Fig. 4 shows the correlation diagram of the bulk energy band and the tight-binding one-electron states of the 55-atom cluster. Filling these states with the number of electrons (210 in the large cluster, 120 in the small) yields the energy gap [the highest occupied–lowest unoccupied molecular orbital (HOMO–LUMO) gap, Fig. 4(centre)]. The resultant clusters have a net charge of −8e on the 55-atom cluster and −4e on the 30-atom cluster [see equation (1)]. The excitation across the HOMO–LUMO gap corresponds to the production of an electron–hole pair, and its energy is modified by the Coulomb interaction between the electron and the hole. The highest hole states (HOMO) are multiply degenerate; this degeneracy is partially lifted by the electron–hole Coulomb interaction [Fig. 4(right)], the effect of which has been calculated *via* degenerate perturbation theory (see Appendix). This calculation yields the first-order Coulomb correction for the energy of the lowest transition, as well as the (triply degenerate) hole wavefunction. With the latter, the relative oscillator strength of this transition is also evaluated. In Fig. 5 we compare the calculated relative intensities of the lowest transitions with experimental absorption spectra of both the 30- and 55-atom clusters (the contribution of cadmium thiophenolate absorption has been subtracted). As can be seen, for the energy of the sharp exciton of the 55-atom cluster the agreement between the calculation (3.66 eV) and the experiment (3.53 eV) is quite good. Furthermore, the calculation correctly reproduces the absence of the exciton-like peak for the smaller 30-atom clusters (Fig. 5), in accord with the experimental observation.

It should be pointed out that the simplicity of the tight-binding model used here (two parameters) allows us to calculate the Coulomb energy correctly using the perturbation approach. With more complex tight-binding models, perturbational calculations become very difficult and therefore, in a previous 13-parameter calculation of CdS clusters,[11] the Coulomb energy was simply estimated from the particle-in-a-box model. Based on the current results, the latter model underestimates the Coulomb energy in the small-cluster regime.

The spatial distribution of the electron and hole wavefunctions is illustrated in Figs. 6 and 7. For the electron wavefunction the square of the normalized amplitude is given on the Cd atoms, the sum of the squares of the three p-state amplitudes is given for the S. For the hole wavefunction the average values of these same quantities are shown, averaged over the three degenerate hole states. For the 30-atom cluster the hole wavefunction is distributed over the four S atoms (labelled S_2) and the electron wavefunction over the six Cd atoms (labelled M_1). For the 55-atom cluster the hole wavefunction is concentrated at the central S atom (S_C, 68%) and the electron wavefunction is mostly delocalized among the 16 Cd atoms (12 M_1, 4 M_F; 70%). This spatial distribution of the wavefunctions is similar to that of the larger (≈40 Å) CdS quantum dot,[13] where the hole wavefunction is smaller than the

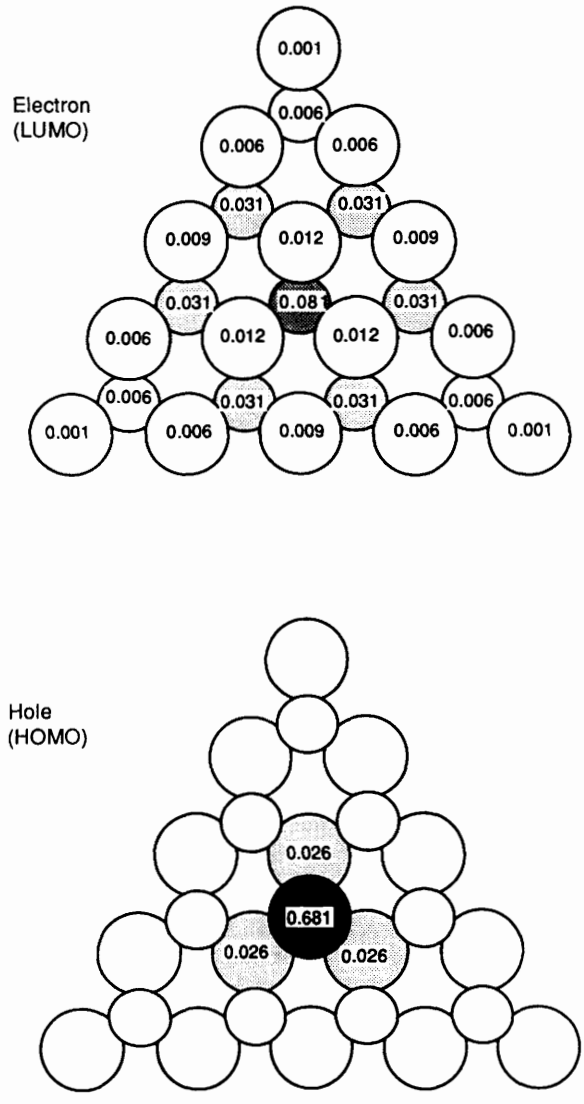

Fig. 6 Lowest electron and hole states of the proposed 55-atom tetrahedral cluster. View shows a face of the tetrahedron (from inside of the cluster for the HOMO and outside for the LUMO) showing the surface S atoms (larger circles) and the next layer of Cd atoms, $\frac{1}{3}$ bond length behind. All other atoms of the cluster are equivalent by symmetry to those shown. Numbers are occupation probabilities of the sites; the shading is a rough depiction of these numbers

electron wavefunction and the maxima of the envelopes of both wavefunctions overlap at the centre of the quantum dot which gives maximum oscillator strength.

Photoluminescence Spectrum.—The low-temperature luminescence and excitation spectra of the 55-atom cluster in a methyltetrahydrofuran–dmf (85:15) matrix are shown in Fig. 8. The excitation spectra (monitored at 440 nm, taken at 18 K) show the same characteristic double peaks as observed in the absorption spectrum. The peak of the luminescence spectrum is Stokes-shifted from the absorption peak by ≈ 5800 cm^{-1} and there are a series of vibronic structures extending towards the absorption peak where, presumably, the 0–0 transition lies. There is no resonant exciton luminescence similar to what has been observed for larger (≈ 40 Å) surface-passivated CdS clusters.[13] This large Stokes shift of the luminescence band indicates that the equilibrium geometry in the excited states is distorted from the ground state, *i.e.* there is strong electron–phonon coupling in the excited state. A closer examination of the temperature-dependent luminescence spectra (Fig. 8) reveals that there are two luminescent bands located at 440

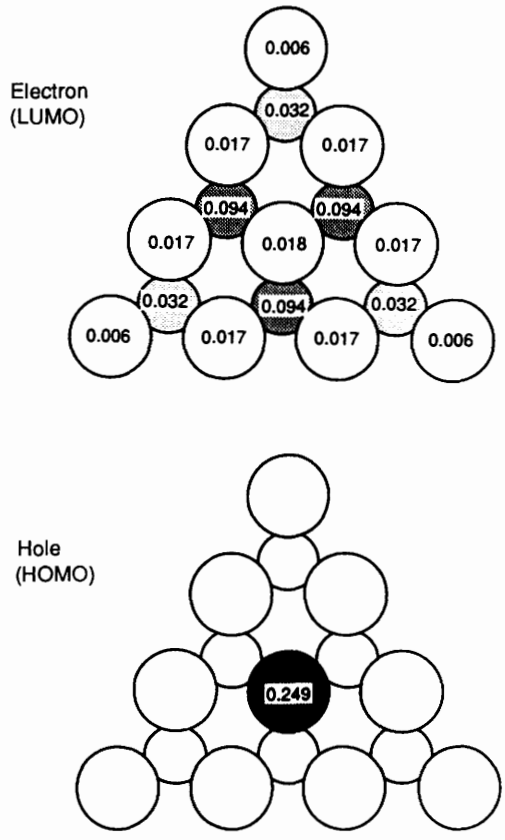

Fig. 7 Lowest electron and hole states of the 30-atom tetrahedral cluster. View shows a face of the tetrahedron (from outside of the cluster) showing the surface S atoms (larger circles) and the next layer of Cd atoms, $\frac{1}{3}$ bond length behind. All other atoms of the cluster are equivalent by symmetry to those shown. Numbers as in Fig. 6

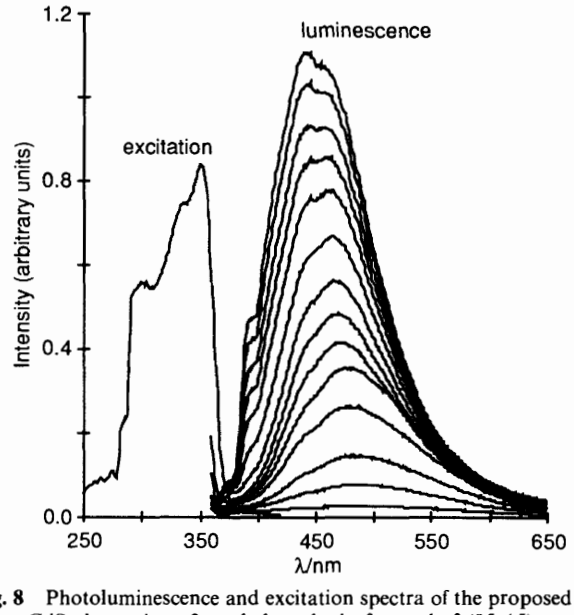

Fig. 8 Photoluminescence and excitation spectra of the proposed 55-atom CdS cluster in a 2-methyltetrahydrofuran–dmf (85:15) matrix. The excitation spectrum (monitored at 440 nm) was taken at 18 K and the photoluminescence spectra at the following temperatures (with decreasing intensities): 25, 35, 45, 55, 65, 80, 100, 120, 140, 160, 180, 200, 228 and 257 K

(2.82) and ≈ 480 nm (2.58 eV). That at 440 nm disappears more rapidly as the temperature rises.

The absorption peak in the excitation spectrum at 18 K is not appreciably narrower than that at room temperature (Fig. 8).

Previously, the homogeneous width for large CdS clusters has been deduced to be ≈ 140 cm^{-1} from a hole-burning study.[14] This indicates that there are factors other than thermal broadening which contribute to the inhomogeneity of the absorption band. The interaction with solvent is a strong possibility. Other possibilities include slight conformational changes among clusters and also defects in the clusters; both can escape the detection of average structure by powder X-ray analysis but would contribute to the broadening mechanism in the absorption spectrum.

Conclusion

Rational synthesis of nanometer-sized semiconductor clusters may be achieved by the linking of two molecular precursors using sulfide ion as cement. A combination of reaction stoichiometry, cluster chemical analysis data, X-ray powder diffractograms and theoretical calculations of spectral properties serves to implicate a structure for the resultant material as a discrete, tetrahedral, $Cd_{20}S_{13}$ core surrounded by thiophenolate ion caps. This results in a soluble quantum-dot material having very sharp absorption features. The exciton of this cluster has a localized hole at the centre of the tetrahedral core and a delocalized electron spread over the entire core leading to maximum oscillator strength. We believe that this approach to cluster synthesis *via* construction of ever larger cluster cores from their smaller precursors may result in a method for producing monodispersed clusters of varying sizes. Such a capability will greatly facilitate the study of both linear and non-linear optical behaviours of semiconductor quantum dots as a function of size.

Appendix

Tight-binding Model for Tetrahedral CdS Clusters.—In this section we give a detailed description of a tight-binding model for calculating the excited electronic states of small tetrahedral CdS clusters. Although a 13-parameter tight-binding description for bulk hexagonal CdS exists in the literature,[15] its application for a cluster would require a very heavy computational load. The accuracy gained thereby would not, however, be justified in view of the known deviations of the bond lengths and angles in tetrahedral clusters, compared to their bulk values. We therefore develop a simplified two-parameter tight-binding model, as follows.

We consider only states composed of 3p orbitals on the S atoms and 5s on the Cd. The difference in on-site energies for these is denoted by Δ. The transfer matrix element between a p state directed along a S–Cd bond and an s state on a neighbouring Cd will be called β. Thus, for example, the matrix element for transfer of a p_x state to its neighbour (and *vice versa*) is given by βe_x, where e is a unit vector along the direction of the transfer. The hexagonal lattice arrangement consists of uniform S–Cd bonds (length $a = 2.52$ Å) directed along the four principal tetrahedral directions, here chosen as the unit vectors.

$$e_1 = (0, 0, 1) \quad \text{(A1)}$$

$$e_2 = [-\sqrt{(2/3)}, -\sqrt{2/3}, -\tfrac{1}{3}] \quad \text{(A2)}$$

$$e_3 = (0, 2\sqrt{2/3}, -\tfrac{1}{3}) \quad \text{(A3)}$$

$$e_4 = [\sqrt{(2/3)}, -\sqrt{2/3}, -\tfrac{1}{3}] \quad \text{(A4)}$$

Corresponding to the four atomic orbitals of the model there are four bulk energy bands. For two of these the linear combination ψ_x of p_x orbitals at wave vector $\boldsymbol{k}$ is given by equations (A5) and (A6) with analogous expressions for ψ_y, ψ_z.

$$\psi_x(\boldsymbol{k}) = \text{constant} \times f_x(\boldsymbol{k}) \quad \text{(A5)}$$

$$f_x(\boldsymbol{k}) \equiv \sum_{j=1}^{4} e_{jx} e^{i\boldsymbol{k}\cdot\boldsymbol{e}_j a} \quad \text{(A6)}$$

The energies of these two bands are the two solutions E of the quadratic equation (A7). The right-hand side of this equation

$$E(E - \Delta) = \beta^2[f_x(\boldsymbol{k})^2 + f_y(\boldsymbol{k})^2 + f_z(\boldsymbol{k})^2] = \beta^2\Big[4 - \frac{4}{3}\cos\Big(\frac{4}{3}k_z a + \frac{\sqrt{2}}{3}k_y a\Big)\cos\Big(\sqrt{\frac{2}{3}}k_x a\Big) - \frac{4}{3}\cos(\sqrt{2}k_y a)\cos\Big(\sqrt{\frac{2}{3}}k_x a\Big) - \frac{2}{3}\cos\Big(\frac{4}{3}k_z a - \frac{2\sqrt{2}}{3}k_y a\Big) - \frac{2}{3}\cos\Big(\frac{2\sqrt{2}}{3}k_x a\Big)\Big] \quad \text{(A7)}$$

vanishes at $\boldsymbol{k} = 0$, at which point the two solutions are $E = 0, \Delta$ and represent band extrema. For small $\boldsymbol{k}$ these bands have equal and opposite curvatures, yielding equal isotropic electron and hole masses [equations (A8) and (A9)].

$$E_{\text{elec}} \rightarrow \Delta + \frac{16\beta^2}{9\Delta}\boldsymbol{k}^2 a^2 \quad \text{(A8)}$$

$$E_{\text{hole}} \rightarrow -\frac{16\beta^2}{9\Delta}\boldsymbol{k}^2 a^2 \quad \text{(A9)}$$

The remaining two energy bands have $E = 0$ independent of $\boldsymbol{k}$; these valence states have p-orbital combinations which for each $\boldsymbol{k}$ are orthogonal to those of the first two bands. The average hole mass at $\boldsymbol{k} = 0$ is the reciprocal of the average of the reciprocal masses of the three valence bands, or exactly three times the mass of the single curved band. Thus the hole mass in this model is three times the electron mass. The experimental value of the electron effective mass in hexagonal CdS is 0.21 electron masses,[16] yielding a value of $\beta = 2.02$ eV. The experimental hole mass is 0.64–0.69,[16] consistent with our simple model. Finally, the parameter Δ in this model must be identified with the bulk band gap, 2.55 eV.[16]

The model yields a 125 × 125 Hamiltonian for the 55-atom tetrahedral cluster (70 × 70 for the 30), the numerical diagonalization of which presents no difficulties. The resulting energy levels are similar to the bulk band structure. For the 55-atom cluster there are 20 states above the gap and 20 below at mirror-image energies of the 20 above; the remaining 85 states are degenerate at the bottom of the gap, $E = 0$. For the 30-atom cluster there are 10 states above and below, 50 degenerate at $E = 0$. A few levels near the gap are given in Fig. 4; energies are in eV, degeneracies are given in parentheses.

We next fill the one-electron levels to the gap: 210 electrons in the large cluster, 120 in the small, and consider the lowest excitation of these many-electron systems. This excitation is the production of an electron–hole pair, and its energy is modified by the Coulomb interaction between the electron and the hole. This Coulomb interaction is strongly screened by the lattice, being describable in a bulk solid by $-e^2/\varepsilon r$ for $r \neq 0$, where e is the charge on the electron, r is the electron–hole distance and ε is the optical relative permittivity (5.5 for CdS). For $r = 0$ (two electrons on the same site), we use the estimate of Sankey and Dow[17] for the electron–electron correlation energies, which gives 9.7 eV for Cd and 12.31 eV for S.

The value of $e^2/\varepsilon a$ (a = bond length, 2.52 Å), 1.04 eV, is small compared to the gap energy, and we expect a perturbative treatment of the Coulomb interaction to be fairly accurate. However, because of the degeneracy of the valence states, degenerate perturbation theory must be used. This at least partially resolves the degeneracy of the hole state. Degenerate perturbation theory for the hole state consists of the diagonalization of an effective Hamiltonian. Let us denote the normalized lowest electron state by $\psi(R)$, where R labels the

particular atom in the cluster as well as the type of orbital for S atoms (*i.e.* p_x, p_y or p_z). The Coulomb interaction, expressed as $V(R,R')$, is of course independent of the orbital label. The effective Hamiltonian is given in matrix notation as in equation (A10) where P is the projection operation into the space

$$\mathscr{H}_{eff} = P \cdot \tilde{V} \cdot P \qquad (A10)$$

spanned by all the degenerate hole states, and $\tilde{V}$ is given by equation (A11). The last term in this expression is the exchange

$$\tilde{V}(R,R') = \delta_{R,R'} \sum_{R''} V(R,R'')\psi^2(R'') \pm \psi(R)V(R,R')\psi(R') \qquad (A11)$$

term; the upper sign applies to a singlet exciton state, the lower to a triplet. Although we included this term in the calculations (for a singlet configuration) its contribution was numerically insignificant.

Eigenvalues of $\mathscr{H}_{eff}$ give the energies by which excited states are lowered below the HOMO–LUMO gap (0.64 eV for the 55-atom cluster and 0.68 eV for the 30-atom cluster). Adding these to the HOMO–LUMO gap gives the transition energies of these excited states.

From the eigenstates of $\mathscr{H}_{eff}$ we can evaluate the oscillator strengths of these transitions in terms of unknown transition-dipole matrix elements. In the spirit of our model, we assume only one non-zero dipole matrix element, for nearest-neighbour transitions with p orbitals of the S atom directed along the Cd–S bond. Oscillator strengths are proportional to the square of the magnitude of the transition dipole. The transition energies and the oscillator strengths (in units of the square of the single unknown transition-dipole matrix element) of these excited states are displayed in Fig. 5(*a*) for the 30-atom cluster and Fig. 5(*b*) for the 55-atom cluster. The energy levels of a few lowest states are listed in Fig. 4.

Acknowledgements

We acknowledge the invaluable technical assistance of Mr. Jack B. Jensen and Ms. Sarah H. Harvey in performing many of the experiments described. We thank Professor J. D. Dow for many useful discussions.

References

1 A. Henglein, *Top. Curr. Chem.*, 1988, **143**, 113; M. L. Steigerwald and L. E. Brus, *Acc. Chem. Res.*, 1990, **183**, 23; Y. Wang and N. Herron, *J. Phys. Chem.*, 1991, **95**, 525 and refs. therein.
2 Y. Wang and N. Herron, *J. Phys. Chem.*, 1988, **92**, 4988.
3 N. Herron, Y. Wang, M. M. Eddy, G. D. Stucky, D. E. Cox, T. Bein and K. Moller, *J. Am. Chem. Soc.*, 1989, **111**, 530.
4 N. Herron, Y. Wang and H. Eckert, *J. Am. Chem. Soc.*, 1990, **112**, 1322.
5 I. G. Dance, A. Choy and M. L. Scudder, *J. Am. Chem. Soc.*, 1984, **106**, 6285.
6 Y. Nosaka, K. Yamaguchi, H. Miyama and H. Hayashi, *Chem. Lett.*, 1988, 605.
7 M. L. Steigerwald, A. P. Alivasatos, J. M. Gibson, T. D. Harris, R. Kortan, A. J. Muller, A. M. Thayer, T. M. Duncan, D. C. Douglass and L. E. Brus, *J. Am. Chem. Soc.*, 1988, **110**, 3046.
8 G. Mills, L. Zongguan and D. Meisel, *J. Phys. Chem.*, 1988, **92**, 822.
9 A. R. Kortan, R. Hull, R. L. Opila, M. G. Bawendi, M. L. Steigerwald, P. J. Carroll and L. E. Brus, *J. Am. Chem. Soc.*, 1990, **112**, 1327.
10 Y. Wang, A. Suna, W. Mahler and R. Kasowski, *J. Chem. Phys.*, 1987, **87**, 7315.
11 P. E. Lippens and M. Lannoo, *Phys. Rev. B*, 1989, **39**, 10935.
12 Y. Z. Hu, M. Lindburg and S. W. Koch, *Phys. Rev. B*, 1990, **42**, 1713.
13 Y. Wang, A. Suna, J. McHugh, E. Hilinski, P. Lucas and R. D. Johnson, *J. Chem. Phys.*, 1990, **92**, 6927.
14 A. P. Alivisatos, A. L. Harris, N. J. Levinos, M. L. Steigerwald and L. E. Brus, *J. Chem. Phys.*, 1988, **89**, 4001.
15 A. Kobayashi, O. F. Sankey, S. M. Voltz and J. D. Dow, *Phys. Rev. B*, 1982, **28**, 935.
16 H. Landolt-R. Bornstein, New Series III/22a, 1988, p. 197.
17 O. F. Sankey and J. D. Dow, *Phys. Rev. B*, 1982, **27**, 7641.

Received 9*th January* 1992; *Paper* 2/00094F